Dynamic Controls on Summit and Flank Eruptions of Basalt

Andrew W. Woods[1], Charlotte Gladstone[1], and Brittain E. Hill[2]

[1]BP Institute for Multiphase Flow, University of Cambridge, Cambridge, CB3 OEZ, England
[2]Center for Nuclear Waste Regulatory Analyses, Southwest Research Institute®,
San Antonio, Texas, USA

Version April 11, 2005

Communicating Author:
Andrew W. Woods
Email: andy@bpi.cam.ac.uk
Phone: 44-1223-765-702
Fax: 44-1223-765-701

ABSTRACT

Many basaltic volcanic eruptions involve the simultaneous discharge of magma from multiple vents with a range of eruption styles and rates including fire-fountaining activity, Strombolian explosions, and effusive lava flows. Here we present a simplified theoretical model for the eruption of basalt through two different vents originating from a common source. The model illustrates how the elevation of the different vents, as well as the distance of the different vents from the common source, controls the significant partitioning of flow between summit or flank vents. Model support is provided by a series of analog laboratory experiments, in which a bubble-liquid mixture ascends multiple conduits using a range of source pressures and gas contents. With a single active vent, the experimental system exhibits flow regimes analogous to Strombolian gas bursts, lava flows, and vigorous fire-fountaining activity, depending on the pressure of the source reservoir and the gas flux. When the bubble-liquid mix simultaneously erupts through both an analog summit and flank conduit, separation of gas from the liquid leads to elevated gas fluxes at the summit vent. Consistent with model calculations, however, the liquid eruption rate through either the flank or the summit vent may dominate, depending on the relative elevation, the relative gas flux, and the reservoir pressure. The model provides a framework for interpreting several field observations of basaltic eruptions with multiple active vents.

1. INTRODUCTION

Basaltic fissure and scoria cone eruptions exhibit a wide variety of eruption styles, including explosive fire-fountaining activity, effusive lava flows, Strombolian gas bursts, and sustained tephra plumes. For some eruptions, multiple vents may be active simultaneously. Although each of the active vents erupts a common magma composition, the vents may have strongly contrasting eruption styles. Many different factors are thought to affect the development of basaltic eruption style, including the geometry of the source reservoir or sill (Vergniolle and Jaupart, 1990), the viscosity and gas content of the magma (Wilson and Head, 1981; Parfitt and Wilson, 1995), the effects of separated gas-liquid flow (Vergniolle and Jaupart, 1986), and the geometry of the dike-conduit system to the surface (Rubin and Pollard, 1987).

Vergniolle and Jaupart (1990) identified how the separation of gas and liquid within the magma reservoir can lead to the formation of a foam within the reservoir. This foam may then coalesce so that large slugs of gas are driven into the conduit periodically, leading to Strombolian gas-burst activity. Gas bubbles supplied from deeper in the system, however, may pass through the foam layer so that a high frequency flux of small bubbles may rise through the conduit. This process leads to a more Hawaiian style of fire-fountaining or bubbly lava flow activity. These experiments identified the importance of the source conditions in generating the different eruption regimes.

Seyfried and Freundt (2000) examined some of the two-phase flow regimes that may develop with separated flow within a volcanic conduit, inspired by Vergniolle and Jaupart's observations of separate liquid and gas fluxes supplied from the magma reservoir. Seyfried and Freundt injected a flux of both gas and liquid at the base of a vertical column initially filled with liquid. In accord with other studies of two-phase flow in a pipe (e.g., Wallis, 1969), Seyfried and Freundt observed a number of different flow regimes in the conduit associated with different gas and liquid fluxes. With a small gas flux, the separation of liquid and gas led to bubbly flow, but with increasing gas flux, slugs developed. At higher gas fluxes, the flow became annular or slug-annular, which is more reminiscent of explosive fire-fountaining type activity.

These studies point to the complex nature of separated two-phase flow and associated effects on overall eruption rates for single conduit systems. Field observations of many basaltic eruptions, however, suggest that the subsurface conduit systems often involve multiple pathways to the surface. For example, Krauskopf (1948) provided detailed observations of the 1943 eruption and deposits at Parícutin, Mexico. Krauskopf postulated that the separation of liquid magma and gas occurred beneath the volcanic edifice and showed how this led to explosive strombolian style activity at the summit, whereas effusive activity occurred at vents located on the flanks of the volcano.

Other observed basaltic scoria cone eruptions also show fire-fountaining to sustained tephra plumes from the summit vent with simultaneous effusion of lavas and spatter from secondary vents near the base of the cone. For example, the 1968 eruption of Cerro Negro volcano in Nicaragua produced a sustained tephra plume from the central vent for 42 days (Viramonte and

Di Scala, 1970). Cone scoria and tephra falls represent the eruption of 13×10^6 m^3 of basalt at a rate of 3.6 m^3 s^{-1}. Coincident with pyroclastic eruptions from the central vent, 7×10^6 m^3 of compositionally identical lavas and spatter erupted from a satellite vent approximately 100 m southwest from the base of the main cone at a rate of 1.9 m^3 s^{-1}. Similar relationships were observed during the Cone 1 stage of the 1975 Tolbachik scoria cone eruption in Russia (Fedotov and Markhinin, 1983). Essentially, the continuous eruption of 190×10^6 m^3 of basaltic magma at a rate of 64 m^3 s^{-1} produced widespread tephra falls from a central vent scoria cone. During the last 11 days of pyroclastic activity at Cone 1, 20×10^6 m^3 of basaltic lavas effused at a rate of 21 m^3 s^{-1} from satellite vents located within 250 m of the base of the cone.

Subsurface fissures that provide flow paths for the magma are strongly controlled by edifice shape and the presence of rift zones. Examples in which there has been eruption from multiple vents on large volcanic edifices include Pu'u 'O'o in Hawaii (Wolfe et al., 1987); numerous episodes of activity at Mount Etna over the past century, especially the more energetic 2001 eruption (Acocella and Neri, 2003); and the 1999–2000 eruptions of Mount Cameroon (Suh et al., 2003). Although the detailed subsurface plumbing system can only be inferred from surface observations, magma likely ascends at depths primarily below the summit of the edifice, then migrates along laterally extensive fissures associated with rifting or faulting (e.g., Fedotov and Markhinin, 1983; Bonaccorso, 2001).

Suh et al. (2003) provided a detailed description of the 1999 and 2000 eruption sequences at Mount Cameroon. Both eruption sequences, which persisted for 20–30 days, involved two areas of activity: a series of high-level vents near the summit of the edifice at 2,650 m and a series of lower-level flank vents at an elevation of 1,500 m. The high-level vents initially effused lavas with an eruption rate of 5.2 m^3 s^{-1} followed by cycles of initial explosive bursts, sustained Strombolian activity, and quiescence. The cyclical activity resulted in scoria cone formation with relatively little lava effusion and erupted 5.1×10^6 m^3 of basaltic magma. In contrast, lower-level flank vents erupted 60×10^6 m^3 of magma predominantly as lavas, with flow rates on the order of 40 m^3 s^{-1}.

Based on the experimental modeling of Seyfried and Freundt (2000) and other work in two-phase flow (e.g., Wallis, 1969; Vergniolle and Jaupart, 1990), the style of activity at flank vents is expected to differ from summit vents as a result of (i) differences in the partitioning of gas and liquid phases along the different pathways to the surface from a common reservoir of bubbly magma, (ii) changes in vent elevation, and (iii) differences in the aperture of the conduits leading to the different vents. To better understand the interrelationships between these processes and resulting effects on eruption characteristics, we will develop a simplified theoretical model for magma flow through a shallow conduit system having summit and flank vents. This model is supported by laboratory experiments using analog bubbly fluids to explore additional effects on flow characteristics from variations in gas content and reservoir overpressure.

2. SIMPLIFIED MODEL OF TWO-PHASE FLOW IN A COMPLEX SUBSURFACE CONDUIT NETWORK

We model the subsurface system of magma flow paths as a primary vertical dike rising from depth, which then branches into summit and flank pathways at a depth of $z = -H$ below the surface (Fig. 1). The bubble-magma mixture is assumed to flow homogeneously along each of the dikes. We assume that the dikes are two-dimensional sheet-like structures, in accordance with general observations that a series of vents associated with both summit and flank eruptions extended for distances on the order of 1 km. Although some flow localization occurs at each vent as the eruption progresses, the initial model uses a one-dimensional representation for each flow path.

In the present investigation, we are concerned with the partitioning of the flow along the vertical and lateral conduits in the shallow subsurface. In this model, the subscripts *f*, *s,* and *t*, denote properties of the flow along the conduits leading to the flank vent, the summit vent, and for the total flow (i.e., below the height $z = -H$), respectively. We assume that the total flow, Q_t, supplied from the deep system partitions into summit and flank fluxes of magma, Q_s and Q_f, while the exsolved gas partitions into mass fractions, n_s and n_f, such that

$$n_t Q_t = n_s Q_s + n_f Q_f \tag{1}$$

We also assume that the dike to the flank vent has inclination, θ, so the effective acceleration of gravity is $g_e = g \sin \theta$, whereas the dike to the summit vent is assumed to be vertical so that $g_e = g$. The distance along the flank fissure to the surface is L, and the elevation of the flank vent is $H–L \tan \theta$ below the summit vent. Because the pressure in the flank and summit conduit is equivalent at the point of intersection, $z = -H$, for simplicity, we assume that these conduits have the same width, w (e.g., Woods et al., 2005). This assumption has an important effect in partitioning the modeled magma fluxes.

Following the original model of Wilson and Head (1981) for the ascent of basaltic magma, the motion of the mixture with speed, u; density, ρ; and viscosity, μ; in a dike of width, w; and pressure, p, is governed by the equations for conservation of momentum and mass. Momentum conservation has the form

$$\rho u \frac{du}{dz} = -\rho g_e + \frac{dp}{dz} - \left(\frac{12\mu}{w^2} + \frac{2C\rho u}{w} \right) u \tag{2}$$

where C is the turbulent friction factor with a value of 0.01 (cf., Woods et al., 2002) and g_e denotes the acceleration of gravity, which depends on the vertical angle of the specific flow path. Conservation of mass is given by

$$\rho u w = Q \tag{3}$$

where Q is the mass flux per unit length of the fissure. The bulk density, ρ, depends on the density of the liquid magma, the gas phase, and the mass of exsolved gas. The density of the exsolved gas may be approximated by the relation p/nRT, where R = 462 J/kg/K for water vapor and R = 182 J/kg/K for CO_2, with a constant temperature, T, of 1,200°C in these calculations. The mass fraction of exsolved gas in the mixture, n, depends on the pressure and the total mass fraction of volatiles in the mixture, n_0. For relatively wet basalt, with 2–4 wt% water (e.g., Nicholis and Rutherford, 2004), we use the approximate relation

$$n(p) = n_o - sp^{1/2} \tag{4}$$

where $s = 3 \times 10^{-6}\,\mathrm{Pa}^{-1/2}$ for basaltic magma, with water being the main volatile phase (Holloway and Blank, 1994). This relationship may represent the original volatile content of the magma if the magma ascends from deep in the crust directly to the surface, or it may represent an elevated volatile content if the magma erupts from a crustal reservoir in which there is already some volatile exsolution owing to volatile accumulation at the top of the reservoir (e.g., Vergniolle and Jaupart, 1990; Phillips and Woods, 2001; Woods and Cardoso, 1997).

Flow is calculated by assuming that for each of the vents, the mixture either decompresses to atmospheric pressure or reaches the local speed of sound for the bubbly mixture and is choked (cf., Wilson and Head, 1981). At the junction between the vertical and lateral conduits, we introduce two equations to account for the pressure change as the magma partitions into the lateral conduit with some horizontal momentum and into the vertical conduit with a reduced vertical momentum flux. Integrating the momentum conservation relations in the vertical and horizontal directions leads to the expressions for the pressure change, Δp_s, from just below the junction where the pressure is $p(-H)$, to where pressure is $p(-H) + \Delta p_s$ for the continuing flow in the vertical conduit and $p(-H) + \Delta p_f$ in the continuing flow in the flank fissure that is given by

$$\Delta p_s = Q_s u_s + Q_f u_f \cos\theta_f - Q_t u_t \tag{5}$$

and

$$\Delta p_f = Q_f u_f \sin\theta_f \tag{6}$$

We have solved these equations for a series of representative total mass fluxes (Fig. 2), which illustrates the partitioning of magma flux between the summit and flank vents as a function of the gas mass fraction in the magma. The pressure changes given by Eqs. 5 and 6 are relatively small compared to the pressure losses resulting from friction in the conduits and the buoyancy forces. For these calculations (Fig. 2), the summit vent elevation is 1,000 m above the flank vent (cf., Mount Cameroon), and the flank vent is supplied by a lateral conduit 1,000 m from the vertical conduit. The source reservoir is located 5 km below the edifice summit, and reservoir pressure is assumed to be lithostatic. For simplicity in the present calculations, we assume that

the source, summit, and flank conduits are all 1 m wide and that flow occurs at a constant temperature.

The additional elevation of the summit vent imposes a substantial impediment to the calculated magma flow, so that even for relatively low gas fractions, the flank vent accounts for more than two-thirds of the magma flux. Even for relatively volatile-rich magmas, the flank vent still accounts for more than half of the magma flux. The change in slope at gas contents greater than 0.03 (Fig. 2) results from flow choking and associated overpressure in the erupting conduit. Because choked flow limits exit velocities to the local speed of sound (e.g., Wilson and Head, 1981), increases in magma flux with gas content are substantially reduced, and there is a reduction in eruption rate from the flank in preference to magma erupting from the summit.

There are several other important controls on the partitioning of magma between summit and flank conduits. The distance of the summit and flank vents from the magma source should affect magma flow partitioning due to the effects of frictional drag in low Reynolds number flow systems such as ascending basalt. The effect of conduit length on flux partitioning is shown in Fig. 3 for model calculations using a variable length for the flank conduit and all other parameters remaining constant. For these calculations, magma flux from the flank vent is equivalent to the flux from the summit vent when the flank conduit is approximately twice the elevation difference between the summit and flank vents (i.e., 2,000 m). Total magma flux also decreases as the length of the flank conduit increases, reflecting the increase in frictional drag along the lengthening pathway to the surface. These calculations show that the geometry of the system has a significant effect on flow partitioning characteristics.

The simplified model assumes magma behaves as a single-phase flow with no slip between the liquid and gas phases. This assumption is not realistic for many volatile-rich basaltic magmas in the shallow subsurface, which likely have different velocities for gas and magma phases (e.g., Vergniolle and Jaupart, 1986). Although the effects of two-phase flow are difficult to evaluate with tractable numerical models, analog experiments can provide useful insights on the effects of gas and magma segregation on flow partitioning.

3. EXPERIMENTAL STUDY

As suggested by the previous calculations, rising magma partitions into different pathways, depending on the difference in elevation between summit and flank vents and the length of each flow path to the surface. The separation of liquid and gas phases along different flow paths, however, also should affect the partitioning of magma between summit and flank vents. Activity at summit vents often involves the eruption of gas-rich magma as tephra plumes or fire fountains. In contrast, magma from the flank vents often occurs as more voluminous eruptions of gas-poor lavas and spatter. These simple observations indicate that separation between gas and magma phases occurs from a common conduit system. To evaluate these phase separation effects, we developed an analog experimental model that captures the first-order effects of simultaneous summit and flank eruptions.

3.1 Apparatus

The experimental system involves a reservoir tank connected to a conduit along a U-tube type structure (Fig. 4a). The plexiglass conduit has a square cross-section of 1 cm^2, which simulates eruption through a single vertical vent. Addition of horizontal sections on top of the vertical section can simulate an eruption through a single flank vent or a simultaneous eruption of the summit and single or multiple flank vents (Fig. 4b). A measured flux of air bubbles is introduced into the base of the supply conduit by either a calibrated peristaltic pump (gas flux 1–25 $cm^3\ s^{-1}$) or pressurized air (gas flux 25–50 $cm^3\ s^{-1}$). Water was used as the working fluid, and in some experiments was dyed red to assist visualization by providing contrast with the bubbles. Fluid overpressure was varied by adjusting the level of water in the reservoir relative to the height of the vents (Fig. 4). The mass of liquid issuing from each vent is recorded as a function of time. Experiments were recorded with digital video equipment.

3.2 Comparison with Basaltic Systems

The experimental system is an analog for the eruption of bubbly basaltic magma and captures many of the important dynamics for two-phase flow of a complex geologic system. Nevertheless, these experiments are conducted at near constant pressure and do not include some of the important effects of decompression, such as gas exsolution and subsequent gas expansion. Thus, gas fraction is approximately constant along the length of the flowing section in the experiment. In addition, some basaltic systems are choked at the vent, whereas the experiments discharge at atmospheric pressure. Although the experiments do not capture the pressure dynamics of choked flow, the phase separation processes related to two-phase flow are analogous to natural basaltic systems.

Bubbles supplied at the base of the supply conduit (Fig. 4) are analogous to either gas produced by volatile exsolution as magma rises through the upper few kilometres in a real magmatic system or gas supplied by deeper exsolution and bubble-liquid separation from the magma reservoir (Vergniolle and Jaupart, 1990; Woods and Cardoso, 1997). In either case, once the gas-magma mixture rises in the conduit, the gas volume fraction increases with decompression. For basaltic magmas with initial water contents of 2 wt%, equilibrium ascent results in bubble formation at depths of approximately 2 km with gas volume fractions >0.9 within 150 m of the surface (i.e., Wilson and Head, 1981). Gas volume also is affected in natural basaltic systems by choking at the vent, initial volatile contents, and the effects of bubble slip during ascent.

In a dike-fed basaltic eruption, the typical flow speeds of the magma are on the order of 1 ms^{-1} with a conduit width on the order 1 m, leading to liquid Reynolds numbers, ul/ν, of value 10–100, where $\nu = \mu/\rho$ is the kinematic viscosity in the range 0.01–0.1 $m^2\ s^{-1}$, given a dynamic viscosity μ = 10–100 Pa s and a density ρ = 2,500 kg m^{-3}. In the experiments, the liquid rises up the vertical section of the experimental conduit with a speed on the order of 1–10 cm s^{-1}. Water has a dynamic viscosity of 10^{-2} Pa s, leading to Reynolds numbers on the order of 10–100 for the experiments, which is comparable to basaltic magma flow. Additionally, the two-phase Reynolds number, which characterizes the two-phase flow regime as defined by Wallis (1969), is on the

order of 10^4–10^5 for both basaltic eruptions and the analog experiments (cf., Seyfried and Freundt, 2000).

In the experiments, gas bubbles are on the order of 1–10 mm in diameter with a rise speed in the range of approximately 1–10 cm s^{-1}; therefore, there may be considerable slip between the bubbles and liquid for low liquid speeds, but less slip will occur at the higher liquid speeds. In a basaltic magma, bubbles derived from gases exsolving from the ascending magma may range in size from 1–10 mm and have rise speeds on the order of 10^{-3}–10^{-1} m s^{-1}. For Strombolian eruptions, larger bubbles produced by coalescence may be on the order of 0.1–1 m in diameter with rise speeds of approximately 1–3 m s^{-1} (i.e., Vergniolle and Jaupart, 1986). The relationships between bubble and liquid rise speeds in the analog experiments appear comparable to these relationships for a range of flow regimes in basaltic eruptions.

The Eotvos number, $\rho g d^2/\sigma$, represents a measure of the importance of surface tension relative to the buoyancy force on the dynamics of bubbles with size d. In the analog experiments, the Eotvos number is approximately 20–30, which indicates that buoyancy forces dominate the effects of surface tension and can lead to bubble deformation. In a basaltic magmatic system, however, the Eotvos number is commonly in the range 10^5–10^7 (Seyfried and Fruendt, 2000), which indicates the buoyancy forces driving the flow are more effective in deforming the bubbles.

3.3 Analog Experiments with Single Vent Systems

Initial experiments were conducted for the ascent of bubble-water fluid through either a single vertical or flank conduit to compare the effects of geometry on simple flow pathways. Additional experiments were conducted using multiple vents that were open to flow concurrently. The pressure of the fluid was varied by changing the depth of water in the reservoir relative to the level of outflow from the vent. Gas supply rate also was varied systematically. Table 1 presents a summary of the various vent geometries used in the experiments and associated experimental results.

3.3.1 Single vertical vent

Initial experiments (Table 1, Series 1) examined the effects of varying gas flux and reservoir pressure on flow regime characteristics on a single vertical conduit. For a reservoir underpressured by 5 cm of vertical depth relative to the top of the conduit and a low gas flux (6 cm^3 s^{-1}), there is a steady release of bubbles but no liquid eruption [Fig. 5a(i)]. As the gas flux increases to 20 cm^3 s^{-1} in the underpressured system, liquid is able to reach the vent and a more vigorous gas-liquid eruption occurs, with bubble coalescence and larger slugs of gas developing in the conduit [Fig. 5a(ii)].

For systems with a neutral reservoir pressure and low gas flux, there is a slow liquid and bubble flow [Fig. 5b(i)]. As gas flux increases to 20 cm^3 s^{-1}, the system flows with similar vigor as the underpressured system [Fig. 5b(ii)]. With the reservoir overpressured by 5 cm of vertical depth,

liquid erupts with no or low gas flux [Fig. 5c(i)]. As the gas flow increases to approximately 10 $cm^3 s^{-1}$, however, the bubbles begin to coalesce and the flow regime becomes more pulsating; larger bubbles rise to the top of the conduit and displace the overlying liquid upward, leading to water fountaining above the vent. As the gas flux increases to 20 $cm^3 s^{-1}$, the gas phase in the conduit becomes more continuous and the flow regime becomes annular (Fig. 5c(ii), cf., Wallis, 1969). Once annular flow occurs, there is little increase in the liquid flux with increasing gas flux because the additional gas is channeled through the center of the conduit.

For an underpressured reservoir, gas bubbles simply rise through the liquid so that there is continual degassing with no liquid eruption until the gas flux reaches a critical value (Fig. 6). As the gas flux increases, the hydrostatic head of the liquid-bubble mixture in the conduit eventually matches the reservoir pressure, and liquid begins to issue from the vent. Initially, liquid flux increases almost linearly with increasing gas flux but declines as bubbles begin to coalesce into a sluggy flow regime. For neutral or overpressured systems, the liquid flux increases with gas flux but at a lower rate than observed for underpressured systems. With increasing reservoir pressure, the liquid flux reaches a nearly constant maximum at a relatively lower gas flux (Fig. 6). This stabilization of a maximum liquid flux corresponds to the development of an annular flow regime and efficient decoupling between gas and liquid flow rates.

3.3.2 Horizontal flank conduit and flank vent

For conduit systems involving a flank vent, gravitational rise of bubbles during horizontal flow can create more complex liquid-gas separation effects than observed in simple vertical conduits. This phase separation occurs rapidly relative to the time of travel along the lateral conduit, which can result in stratification of the horizontal flows. For low gas fluxes (i.e., 6 $cm^3 s^{-1}$), bubbles travel over the liquid surface as a fully separated flow, although the continuing flux of gas does drive some liquid along the conduit (Table 1, Series 2). These bubbles may coalesce [Fig. 7a(i)] for underpressured systems, but may remain discrete for some neutral pressure systems [Fig. 7b(i)]. As the gas flux increases to 30 $cm^3 s^{-1}$, the flow remains separated, although there is some frictional coupling between the liquid and gas at the interface that leads to small wave formation on the surface of the liquid. With increasing gas flux, these waves become much larger and can break, leading to some mixing of the gas and liquid phases in the lateral section of the conduit. This mixing is primarily caused by the development of large slugs or bubbles of gas [Figs. 7a(ii) and 7b(ii)].

Relationships between liquid flow rate and gas flux for the lateral conduit geometry are very similar to relationships observed for a vertical conduit. As expected, a critical gas flux is required to initiate liquid flow in an underpressured system (Fig. 8). Comparison with Fig. 6 indicates that for overpressured or neutrally pressured reservoirs, liquid flow as the gas flux increases in vertical conduits is 10–20% greater than in lateral conduits. This reduction in the liquid flux for lateral conduits results from stratification of the flow, which reduces the coupling between gas bubbles and liquid to a greater extent than occurs in vertical conduits. When the vertical conduit is underpressured, however, the liquid flow through the vertical conduit is comparable to that through the lateral dike. This relationship occurs because the gas flux is

required only to reduce buoyancy sufficient to drive liquid up the supply conduit to the level of the lateral conduit. In this vertical conduit, the flow is not stratified (Fig. 7).

To more realistically simulate a volcanic eruption, additional experiments were conducted with a 3-cm vertical section added to the exit point of the lateral conduit (Fig. 4; Table 1, Series 3). This short section allowed liquids to accumulate periodically in this vertical section for experiments conducted with larger gas fluxes. The liquid accumulations briefly prevent the gas bubbles from flowing out of the lateral conduit, although some gas vents from the system during early stages of liquid accumulation. Liquid flux is gradually reduced and eventually ceases. When sufficient gas pressure has accumulated, a liquid slug is forced out of the conduit and the gas is released. This process creates rapid periodic cycles in which liquid fills and then erupts from the vertical section at the end of the lateral conduit.

3.4 Analog Experiments with a Double Vent System

The single vent experiments described above demonstrate some of the flow characteristics that can be modeled with a simple analog experiment. Many basaltic volcanoes, however, have simultaneous eruptions of both summit and one or several flank vents. This geometry can be modeled with the experimental apparatus, with the height of the vertical conduit greater than the level of the lateral vent (Fig. 4b). The reservoir pressure was neutrally balanced throughout these experiments relative to the near-flank vent. Thus, the summit vent was underpressured when opened, and the far-flank vent was overpressured when opened.

One important difference between these experiments and the earlier single vent experiments is that the gas flux and liquid flux may be partitioned into different proportions because of differences in motion for the gas bubbles relative to the liquid. At the junction between the conduits to the summit vent and the flank vents, the gas flux is expected to partition preferentially into the summit conduit. The liquid flux, however, may partition in different proportions depending, for example, on the elevation of the summit vent relative to the flank vent and the reservoir pressure. This partitioning can lead to very different styles of activity at the summit vent and the flank vent in the experimental system.

3.4.1 Interaction of the summit vent and a single flank vent

A summit conduit was used as an analog to summit-flank vents on volcanoes, with a vent 6.2 cm above the level of the flank vent that corresponded to the level of neutral pressure in the experimental system (Table 1, Series 4). For gas fluxes <10 $cm^3\ s^{-1}$, liquid eruption from the summit vent was suppressed and liquid only erupted from the flank vent (Fig. 9a). There was, however, a steady stream of gas bubbles that separated from the liquid at the junction between the summit and flank conduits. These bubbles then erupted from the summit vent, leading to periodic bubble bursting that is reminiscent of Strombolian activity. During these bursts, some liquid did rise up the summit conduit, but did not reach the vent (Fig. 9a). Simultaneously, the flank vent effused a relatively gas-poor liquid, analogous to lava flow activity. Although the flank conduit contains gas-poor liquid, the main conduit below the junction that supplies the

flank and summit vents contains a more bubbly liquid with a relatively lower bulk density. Thus, the pressure gradient in the main conduit is less than hydrostatic. The pressure at the junction with the flank conduit is, therefore, greater than the pressure at the base of the main conduit, excluding the hydrostatic pressure difference between the base of the conduit and the junction. If this increase in pressure at the inflow to the flank conduit is sufficiently high, liquid can flow along the flank conduit to the surface. This flow can occur even if the liquid migrating along the flank is bubble-poor and if there is no concurrent eruption of liquid from the summit vent.

As the gas flux increases, the gas content of the main conduit increases below the junction with the flank conduit. This increases the pressure at the junction and increases the depth of the liquid layer within the summit conduit above the junction (Fig. 9b). Additionally, since the pressure at the junction increases, more liquid then flows along the flank conduit. This increased flow rate captures a greater flux of gas bubbles, producing more vigorous, fire-fountaining type activity at the flank vent (Fig. 9b). Because the liquid and gas flux along the flank conduit is increased, larger slugs of gas can form and tend to fill the cross-sectional area of the flank conduit. As the gas flux increases, the liquid also reaches a greater height in the summit conduit, although it does not reach the summit vent for the range of gas fluxes used in these experiments.

The relative height of the flank vent and the summit vent is an important factor in determining the style of effusion observed in the experiments. This effect is expected given the changes in liquid eruption rates in the single vent experiments for associated changes in reservoir pressure. To evaluate this effect further for multiple vent geometries, the height of the summit vent was reduced to 2 cm above the height of the flank vent (Table 1, Series 5). With the lower summit height, liquid as well as gas was able to erupt from both vents at lower gas fluxes than for a 6.2-cm high summit (Fig. 9c). As the gas flux increased, a greater proportion of the liquid erupted from the summit vent rather than from the flank vent, because bubbles rising directly to the surface draw liquid upwards (Fig. 9d). The liquid flux through both vents, however, increases with increasing gas flux (Fig. 10a). For gas fluxes <10 cm^3 s^{-1}, all of the liquid flow is through the flank vent. Total liquid flow increases with increasing gas flux until liquid reaches the level of the summit vent. Subsequently, as the gas flux increases, a progressively larger fraction of the erupting liquid issues through the summit vent with an associated decrease in liquid flux through the flank vent (Fig. 10a). Eventually the liquid flux is dominated by the flow through the summit vent. As the total gas flux increases, however, the total eruption rate also increases, although at a significantly lower rate.

Additional experiments were conducted with the summit vent and a far-flank vent (Fig. 4b) with the near-flank vent closed (Table 1, Series 6), to evaluate the influence of pathway length on gas segregation and flow processes. Using this configuration, the elevation difference between the two vents was set to 4 cm or 8.2 cm. Very similar flow regimes were observed as found in the previous experiments, although the critical gas flux required to raise liquid in the summit conduit and induce flow was greater (Fig. 10b). This difference occurred because the increase in pressure from friction in the far-flank vent resulted in liquid preferentially erupting through the flank instead of the summit. As a result, the maximum flux of liquid from the flank vent was greater and occured at a critical gas flux when liquid reached the summit vent. As the gas flux increases

beyond this critical value, the fluid flux from the flank vent decreases, whereas the overall liquid flow slowly increases as it also exits the summit (Fig. 10b).

3.4.2 Interaction of two flank vents supplied by a horizontal conduit

If the summit vent is plugged, multiple vents potentially can open on the flank of a volcano. For this configuration (Table 1, Series 7), liquid and gas were able to vent from both flank vents (Fig. 9e). Due to the stratification of the bubble-liquid mixture as it moved along the horizontal flank conduit, however, most of the bubbles vented from the near-flank vent, even though the far-flank vent had a lower elevation (Fig. 9e). This condition led to more vigorous fountaining-style activity from the near-flank vent, whereas a gas-poor flow effused from the far-flank vent. Because the far-flank vent has a relatively lower elevation, approximately 70–80% of the total liquid flux occurred from the far-flank vent regardless of gas flux (Fig. 10c). This result is different from previous observations where the liquid flux undergoes a transition from flank dominance to summit dominance as the gas flux increases (e.g., Fig. 10a).

3.5 Generalized Numerical Model

The wide range of flow regimes observed in the analog experiments illustrates the significant effects of two-phase flow and geometry of the conduit system on the development of flow dynamics and phase partitioning. A simplified model for flow, which uses an average buoyancy representation of the gas-liquid mixture (e.g., Wallis, 1969), can provide insights on the processes that affect flow characteristics in the analog system. For a given gas flux, Q_G, the experiments show a time-averaged value for the liquid flux, Q_L, and the gas content, ϕ, averaged along the conduit. As a result, assuming that the density of air is negligible compared to water, the buoyancy force driving the flow is given by

$$\Delta p = \rho_L g \varphi (H - h) - \rho_L g (1 - \varphi) h \tag{7}$$

where the first term is the difference between the weight of the bubbly mixture in the conduit for depth $H-h$ and the weight of pure liquid in the reservoir for depth $H-h$, and the second term denotes the weight of the bubbly mixture in the part of the conduit above the level of fluid in the reservoir, of depth h, which tends to oppose the flow. If there is no eruption of liquid, as occurs for low gas fluxes with an underpressured reservoir (e.g., Figs. 9a and 10a), the net buoyancy force is zero. Thus, the bubble content of the liquid in the conduit is related to the depth of the liquid according to the relation

$$\varphi H = h \tag{8}$$

As anticipated, a higher vent requires a larger gas flux to drive an eruption of liquid. This process can be expressed in terms of the void fraction of gas in the conduit required to drive a flow

$$\varphi > h / H \tag{9}$$

If the condition that the bubble-liquid mixture reaches the top of the conduit and Eq. 9 is satisfied, the liquid flux is given by the balance between the buoyancy force and the viscous or turbulent dissipation.

In the analog experiments, the rise speed of isolated gas bubbles that fill the conduit scales as $0.4(gw)^{1/2}$ with a conduit of width w = 1 cm (Clanet et al., 2004). For the experimental condition, calculated rise speed is approximately 0.13 m s^{-1}, which is consistent in order of magnitude with observed rise speeds. Nevertheless, considerable variation occurred in the rise speed of individual bubbles owing to variations in bubble size and also due to bubble-wake and bubble-bubble interactions (cf., Campos and Guedes de Carvalho, 1988). For a liquid flux of order 1–40 $cm^3 s^{-1}$, as measured in many of the experiments, the volume flux per unit area of conduit (i.e., transport velocity) was 0.01–0.4 m s^{-1}. This velocity spans the range of rise speeds for bubbles relative to the liquid. With small gas fluxes, the liquid flux is small. Thus, bubbles rise through the liquid and produce a separated bubbly flow. In this flow regime, bubble size is determined by the dynamics of bubble separation from the source. Bubbles essentially grow until their rise speed exceeds the rate of expansion of the bubble resulting from the continuing influx of gas at the source. As the gas flux increases, the bubbles become larger and the void fraction of the conduit increases. The associated increase in buoyancy force then drives a larger liquid flux. The flow thus evolves from the bubbly regime, through a large gas-slug regime in which the gas and liquid velocities are similar, and to an annular regime in which a nearly connected gas phase develops throughout the conduit (e.g., Wallis, 1969).

In the case of a double vent system, partitioning of the gas flux between the vents is important for determining eruption rates from each vent. Equation 7 indicates, in a simplified way, that the pressure driving the liquid flux decreases when the elevation of the vent increases or the void fraction decreases. To achieve comparable liquid eruption rates through two vents of different elevation having conduits of comparable geometry, there should be a comparable pressure driving the flow. Hence, the higher vent requires a larger gas fraction, and thus a greater gas flux. This effect is shown in Fig. 11, which shows the variation of gas content as a function of vent elevation in order to produce a given buoyancy force on the liquid in the conduit. Gas fractions in the range 0.1–0.4 are required to provide net buoyancy forces (Fig. 11). Visual observation suggests that void fractions were in this range for many of the experiments (Fig. 9). We, therefore, infer that the pressure driving the experimental flows was equivalent to water a few centimeters deep.

It is interesting to calculate whether a balance of such a buoyancy force with the viscous and turbulent stresses exerted by the walls of the conduit leads to predictions of flow rate comparable to the experimental observations. The force balance may be expressed in the simplified form for homogeneous flow, given by Eq. 1, as

$$\frac{12\mu u}{w^2}\left(1+\frac{f\rho dw}{12\mu}\right)=\frac{\Delta p}{L} \tag{10}$$

where Δp is the net buoyancy force given by Eq. 7 and L is the length of the conduit. If the buoyancy force driving the flow is comparable to the hydrostatic pressure of 1–5 cm of water, corresponding to void fractions on the order of 0.1–4.4, then Eq. 10 implies flow speeds of 0.1–0.5 m s^{-1}. Note that in these calculations, the local length scale of viscous and turbulent dissipation is assumed comparable to the width of the conduit, w. This simplified estimate of the flow speed is in accord with the observations of liquid fluxes of 10–50 $cm^3 s^{-1}$, confirming the applicability of the simplified homogeneous flow model for higher liquid and gas fluxes.

4. DISCUSSION

From the experimental results, the partitioning of the gas flux between the summit vent and the flank vent depends on the geometry of the source conduit (e.g., Figs. 9a and 9e). In many cases, the summit vent tends to localize much of the gas flux. Our experiments and the theoretical calculations of Section 2 identify, however, that either the summit or the flank vent may conduct the majority of the liquid flow, depending on the pressure and gas flux in the source magma and the difference in elevation of and distance to the summit and flank vents. With a large difference in elevation, the experimental models show that it is possible to have small liquid eruption rates and relatively large gas fluxes at the summit vent. This condition appears analogous to Strombolian type eruptions, as documented at Mount Cameroon, with the flank vent effusing large volumes of lava flows or even fire-fountaining activity.

The dynamics of the two-phase flow are difficult to constrain quantitatively because the partitioning of the gas phase may change significantly in conduit systems with differing geometry. In addition, flow dissipation in the conduit depends critically on the flow regime, and the relevant boundary condition at the vents depends on the degree of separation of the gas and liquid flow; hence, the appropriate speed of sound when the mixture is overpressured (e.g., Wallis, 1969). Nevertheless, it is possible to gain some useful insights by turning to the parameters appropriate for magma at volcanoes and then evaluating the magmastatic pressure distribution along the summit and flank conduits, including the effect of any bubbles mixed into the flow (e.g., Fig. 11).

Magmastatic pressure can be calculated as a function of the vertical distance above the junction between the flank and summit conduits for a range of gas contents in an idealized magmatic system (Fig. 12). In these calculations, the pressure at the junction is simplified as lithostatic, and the magma-gas mixture is allowed to expand above this point. As the gas content increases, the pressure becomes progressively more elevated relative to lithostatic at each height above the junction. If more bubbles ascend through to the summit conduit than the flank conduit, the overpressure should become higher in the summit conduit and lead to increased magma flow even though the vent is at higher elevation. This calculation is consistent with the analog

experiments, which show that progressive increases in the gas flux led to an increasing fraction of the liquid flow being erupted from the summit vent at the expense of the flank vent.

The homogeneous flow model that was introduced in Section 2 can be extended to evaluate flank vent geometries that are more realistic than a horizontal conduit (i.e., Fig. 1). This model evaluates magma eruption rates at the summit vent and the flank vent as a function of gas flux at that vent for magma rising from a common source 1 km below the summit at pressure close to lithostatic. The flank vent can be inclined 30°, 60°, and 90° to the summit vent, with lengths of the flank conduits chosen to intersect a large volcanic edifice of slope 30° relative to horizontal. For relatively low gas fluxes, magma flow is dominated by the lateral flank conduits with shallower angles (Fig. 13). With increasing gas flux, however, buoyancy tends to increase the fraction of the flow moving along the vertical conduit, which leads to a reversal in the flow, and more material erupts from the vertical or steeper conduits than the lateral conduits (Fig. 13).

In contrast to Mount Cameroon, elevation differences between summit vents and satellite vents at basaltic scoria cones are on the order of 100–200 m. These relatively small elevation differences appear more analogous to the near-flank and far-flank experiments (Fig. 10c) than summit and flank vent experiments (Fig. 10a). Although these experiments showed significantly larger flow rates for the far-flank vent, the basaltic scoria cone eruptions show that larger flow rates can occur from the near-flank vent (i.e., central scoria cone vent). If the fluid pressure in the experiments was lowered below the level of the far-flank vent or the horizontal conduit was inclined toward the supply conduit, the far-flank vent would not flow until an appreciable gas flux reached the vent. Because the near-flank vent effectively captured the segregated gas bubbles, the far-flank vent could not flow. Gas bubbles are not separated from an erupting basaltic magma with the same efficiency as air bubbles from flowing water. Lava effusion could occur from the scoria cone satellite vents as gas bubbles continue to evolve from the magma after separation from the supply conduit at depth.

5. SUMMARY

The dynamics of basaltic eruptions in a multivent eruptive system were evaluated using a series of simplified theoretical models and analog laboratory experiments. Although simplifying assumptions were used, the models provide useful insights into the controls on eruption style and flow regime for summit and flank vents. The general principles suggested by the simplified theoretical models and experiments were that with a summit vent and a flank vent, the important controls on the relative eruption rates are the volatile content of the magma, the partitioning of these volatiles between the summit and flank conduits, and the elevation and distance of the flank vent relative to the summit vent. With higher gas fluxes, the summit vent tends to become more active and is the site of vigorous fountaining activity. If, however, the summit vent is significantly higher than the flank vent, there may be considerable degassing from the summit vent with some Strombolian style explosions, but little liquid is erupted. Concurrently, the flank vent may become the locus of magma eruption, with either voluminous lava flows or milder fire-fountaining activity occurring depending on the gas flux and separation of the gas from the magma within the conduit.

These observations of different eruption styles from different vents, which are all supplied from the same source, provide some rationale for the numerous field observations of different eruption styles during basaltic eruptions, such as at 1999–2000 Mount Cameroon (Suh et al., 2003), numerous eruptions of basaltic scoria cones, and during fissure eruptions in Hawaii.

Nevertheless, although some general principles emerge from the present study and the qualitative behavior of the experiments and model is analogous to some field observations, some important simplifying assumptions were made necessarily in this investigation. Factors that are also likely to be important in controlling the dynamics of summit and flank eruptions include: (i) conduit geometry; (ii) relative aperture of the summit and flank conduits; and (iii) distribution of bubbles within the ascending magma-gas mixture, which are likely to be much smaller than the conduit aperture (in contrast to our small-scale experiments) and will have a key influence on the partitioning of the gas between the conduits. Also, the present analog laboratory models do not account for effects of gas exsolution and expansion within the conduit, which also are likely to have an effect on the quantitative controls of partitioning of the gas flux. The present work does, however, provide a useful but simplified framework that illustrates some of the controls on the simultaneous eruption of basalt from different vents, which builds on the classical work of Krauskopf (1948).

Acknowledgements

This paper was prepared to document work performed by the Center for Nuclear Waste Regulatory Analyses (CNWRA) for the U.S. Nuclear Regulatory Commission (NRC) under Contract No. NRC–02–02–012. The activities reported here were performed on behalf of the NRC Office of Nuclear Material Safety and Safeguards, Division of High Level Waste Repository Safety. This paper is an independent product of the CNWRA and does not necessarily reflect the view or regulatory position of NRC.

References

Acocella V, Neri M (2003) What makes flank eruptions? The 2001 Etna eruption and its possible triggering mechanisms. Bull Volcanol 65:517–529.

Bonaccorso A (2001) Mt Etna volcano: Modeling of ground deformation patterns of recent eruptions and considerations on the associated precursors. J Volcan Geotherm Res 109:99–108.

Campos J, Guedes de Carvalho, J (1988) An experimental study of the wake of gas slugs rising in liquids. J Fluid Mech 196:27–37.

Clanet C, Heraut P, Searby G (2004) On the motion of bubbles in vertical tubes of arbitrary cross-sections: some complements to the Dumitrescu-Taylor problem. J Fluid Mech 519:359–376.

Fedotov SA, Markhinin YeK (1983) The Great Tolbachik Fissure Eruption, Geological and Geophysical Data 1975–1976. Cambridge University Press, New York, 353 pp.

Holloway JR, Blank JG (1994) Application of experimental results to C-O-H species in natural melts. In: Carroll MR, Holloway JR (eds) Volatiles in Magmas, Reviews in Mineralogy 30:187–230. Washington, DC: Mineralogical Society of America.

Krauskopf KB (1948) Lava movement at Parícutin volcano, Mexico. Geol Soc Am Bull 59:1267–1283.

Parfitt E, Wilson L (1995) Explosive volcanic eruptions IX. The transition between Hawaiian style lava fountaining and Strombolian explosive activity. Geophys J Int 11:226–232.

Phillips JC, Woods AW (2002) Suppression of large scale magma mixing by melt volatile separation. Earth Planet Sci Lett 204:47–60.

Rubin AM, Pollard DD (1987) Origin of blade-like dikes in volcanic rift zones. US Geol Surv Prof Pap 1350:537–570.

Nicholis MG, Rutherford MJ (2004) Experimental constraints on magma ascent rate for the Crater Flat volcanic zone hawaiite. Geology 32:489–492.

Seyfried R, Fruendt A (2000) Experiments on conduit flow and eruption behaviour of basaltic volcanic eruptions. J Geophys Res 105:23727–23740.

Suh, CE, Sparks RSJ, Fitton JG, Ayonghe SN, Annen C, Nana A, Luckman A (2003) The 1999 and 2000 eruptions of Mount Cameroon, eruption behaviour and petrochemistry of lava. Bull Volcanol 65:267–281.

Vergniolle S, Jaupart C (1990) Dynamics of degassing at Kilauea Volcano, Hawaii. J. Geophys Res 95:2793–2809.

Vergniolle S, Jaupart C (1986) Separated two-phase flow and basaltic eruptions. J Geophys Res 91:12842–12860.

Viramonte JG, Di Scala L (1970) Summary of the 1968 eruption of Cerro Negro, Nicaragua. Bull Volcanol 34:347–351.

Wallis GB (1969) One dimensional two phase flow. McGraw Hill, New York, 408 pp.

Wilson L, Head J (1981) Ascent and eruption of magma on Earth and the Moon. J Geophys Res 86:2971–3001.

Wolfe EW, Garcia MO, Jackson DB, Koyanagi RY, Neal CA, Okamura AT (1987) The Pu'u 'O'o eruption of Kilauea volcano, episodes 1–20, January 3, 1983 to June 8, 1984. US Geol Surv Prof Pap 1350:471–508.

Woods AW, Cardoso SSS (1997) Bubble-magma separation and the triggering of basaltic volcanic eruptions. Nature 385:518–520.

Woods AW, Sparks S, Bokhove O, Lejeune A-M, Connor CB, Hill BE (2002) Modeling magma-drift interaction at the proposed high-level radioactive waste repository at Yucca Mountain, Nevada, USA. Geophys Res Lett DOI 10.1029/2002GL014665.

Woods AW, Bokhove O, de Boer A, Hill BE (2005) Compressible magma flow in a two-dimensional elastic-walled dike. Earth Planet Sci Lett (in press).

Figure Captions

Figure 1. Schematic cross section of the shallow conduit system for a representative basaltic volcano having summit and flank vents that originate from a common supply conduit.

Figure 2. Calculated mass eruption rate for magma rising along a 1-m wide vertical conduit from a 5-km deep reservoir. Conduit divides at 1 km depth into a 1-m wide horizontal conduit extending 1 km to a flank vent and a 1-m wide vertical conduit extending to the summit vent.

Figure 3. Calculated mass eruption rate for same conditions as Figure 2, except length of horizontal flank conduit varies from 1,500–4,000 m and gas fraction is fixed at 0.03.

Figure 4. Schematic of apparatus used for analog experiments. (a) Overall configuration showing relationship between reservoir and a single vent and (b) detail of vent system showing expansion of vent system to use multiple flank vents.

Figure 5. Representative images of different flow regimes for vertical conduit experiments. Series (i) conducted with a gas flux of 6 $cm^3\ s^{-1}$ and Series (ii) with a gas flux of 30 $cm^3\ s^{-1}$. (a) Fluid system is underpressured, (b) system is at neutral pressure, and (c) system is overpressured.

Figure 6. Relationship between gas flux and erupted liquid flux for experiments with a single vertical vent. Changes in eruption rate with increasing gas flux reflect evolution of the flow regime from bubbly, to slug, to slug-annular, to annular.

Figure 7. Representative images of different flow regimes for selected horizontal conduit experiments. Series (i) conducted with a gas flux of 6 $cm^3\ s^{-1}$ and Series (ii) with a gas flux of 30 $cm^3\ s^{-1}$. (a) Fluid system is underpressured and (b) system is at neutral pressure.

Figure 8. Relationship between gas flux and erupted liquid flux for experiments with a single horizontal conduit and vent (Fig. 7). Changes in eruption rate with increasing gas flux reflect evolution of the flow regime from bubbly, to slug, to slug-annular, to annular.

Figure 9. Representative images of different flow regimes for multiple conduit experiments. All experiments conducted with neutral fluid pressure at elevation of the near-flank vent. (a) Summit vent 6.2 cm above single flank vent, gas flux of 12.2 $cm^3\ s^{-1}$; (b) is equivalent to (a) except gas flux increased to 43.3 $cm^3\ s^{-1}$; (c) summit vent reduced to 2 cm above flank vent, gas flux of 16 $cm^3\ s^{-1}$; (d) is equivalent to (c) except gas flux increased to 40 $cm^3\ s^{-1}$; and (e) summit vent closed, near vent is 2 cm higher than far vent, gas flux of 16 $cm^3\ s^{-1}$.

Figure 10. Relationship between gas flux and liquid eruption rate for experiments with multiple conduit and vent configurations (cf., Fig. 9). For configuration (a–b), Q_T is the total liquid flux, Q_S is the flux of liquid from the summit vent, and Q_F is the flux of liquid from the flank vent. For

configuration (c), Q_N is the liquid flux from the near-flank vent and Q_F is the liquid flux from the far-flank vent.

Figure 11. Calculation of the void fraction required to produce a net pressure on the liquid equivalent to a given depth of water (labeled curves) as a function of vent height above the level of the fluid reservoir.

Figure 12. Calculation of the overpressure in a magmastatic column as a function of height above a reservoir located 3 km below the surface at lithostatic pressure. Curves are shown for mass fractions of volatiles at 2 wt%, 3 wt%, and 4 wt%. If the gas partitions into different fractions in the summit and the flank conduits, then the overpressure in each conduit will be different at a given height. Even if the summit vent is higher than the flank vent, the overpressure may be larger if more gas rises into the summit conduit. For this condition, there will be a greater liquid flux issuing from the summit vent.

Figure 13. Calculation of the eruption rate from a shallow reservoir along both a vertical conduit rising 1 km to the summit (solid line) and a conduit that extends laterally from the reservoir at angles of 30°, 60°, or 90°. The flank vents are assumed to intersect the volcanic edifice at an angle 30° (Fig. 1). Curves are shown for different values of gas content. If the gas is partitioned so that more gas rises to the summit vent, then a greater eruption rate will occur at the summit. For a relatively smaller gas content in the magma, eruption at the flank vent is preferred because of the lower elevation of the vent.

Table 1. Summary of analog experiments using single vents (Series 1–3) and multiple configurations of double vents (Series 4–7).

Series	**Model Configuration**	**Images**	**Eruption Data**
Single Vent Experiments			
1	Vertical conduit only	Figure 5	Figure 6
2	Horizontal flank	Figure 7	Figure 8
3	Flank with vertical exit point	n/a	n/a
Multiple Vent Experiments			
4	Tall summit vent + Near-flank vent	Figures 9a, 9b	n/a
5	Short summit vent + Near-flank vent	Figures 9c, 9d	Figure 10(i)
6	Short summit vent + Far-flank vent	n/a	Figure 10(ii)
7	Near-flank vent + Far-flank vent	Figure 9e	Figure 10(iii)

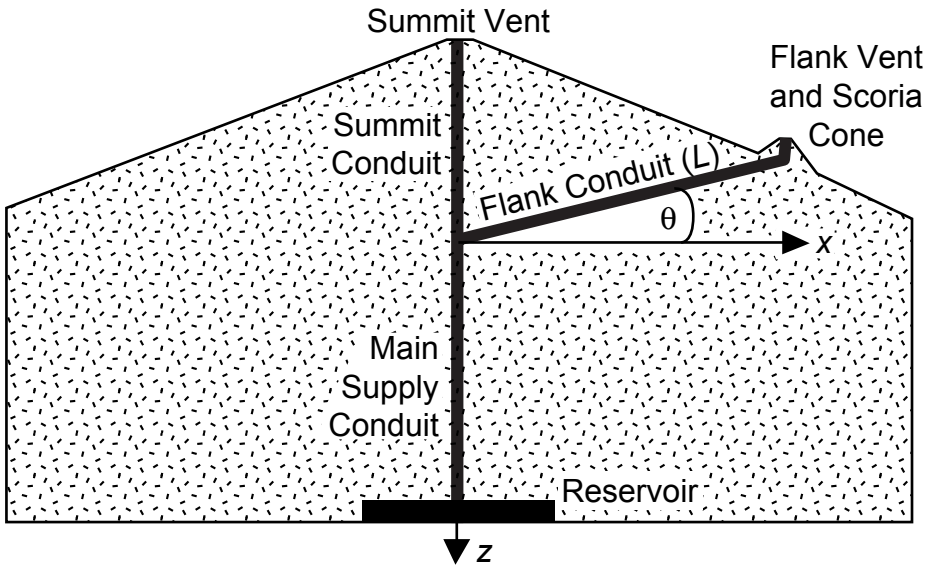

Figure 1, Woods et al., 2005

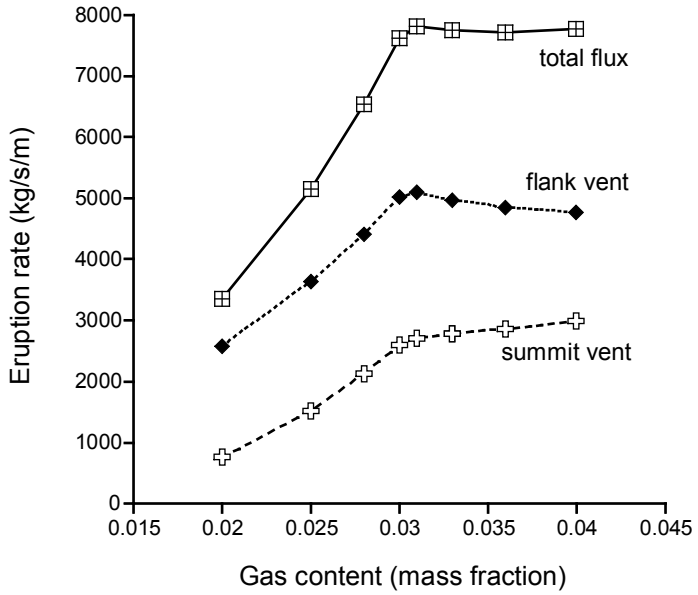

Figure 2, Woods et al., 2005

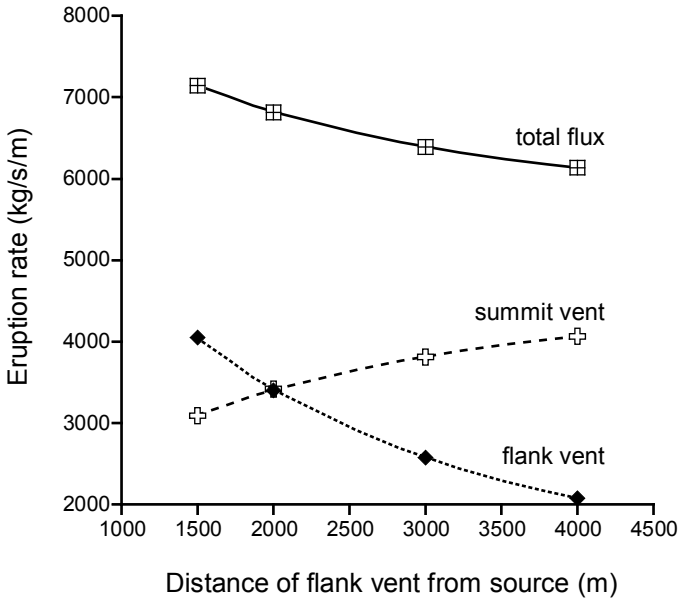

Figure 3, Woods et al., 2005

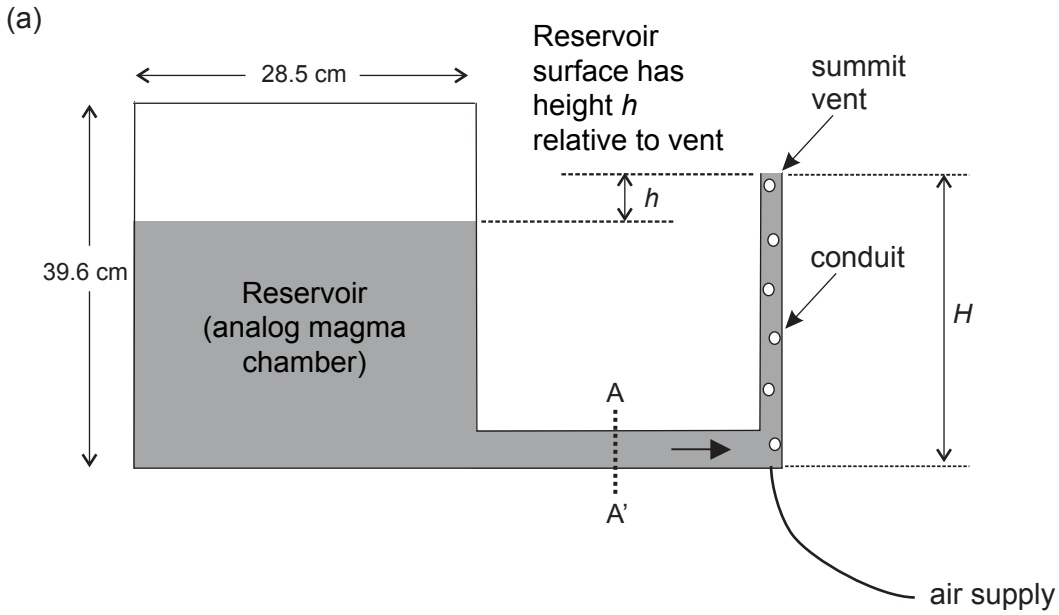

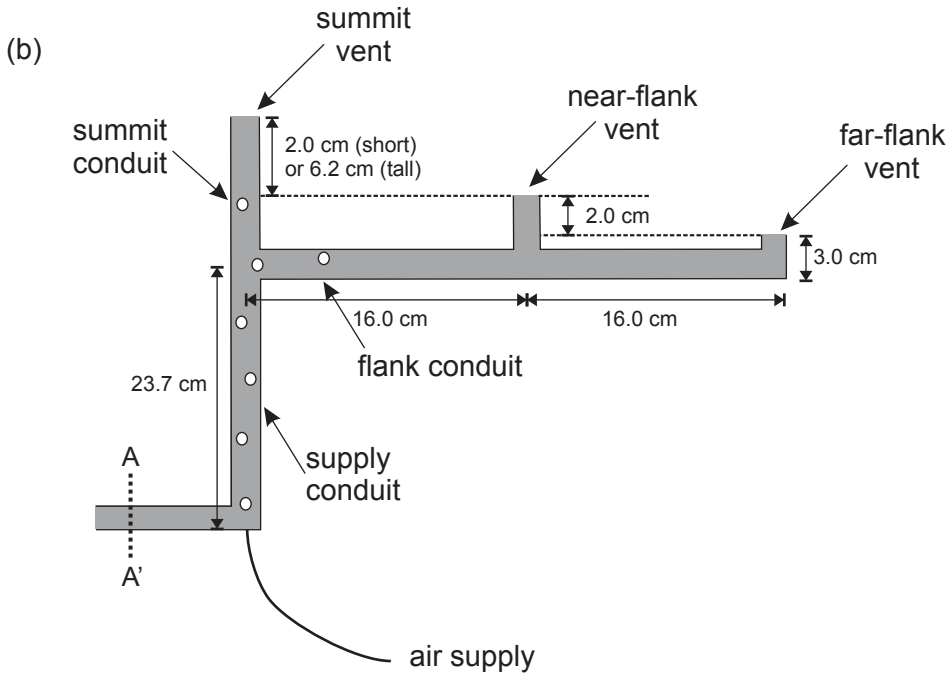

Figure 4, Woods et al., 2005

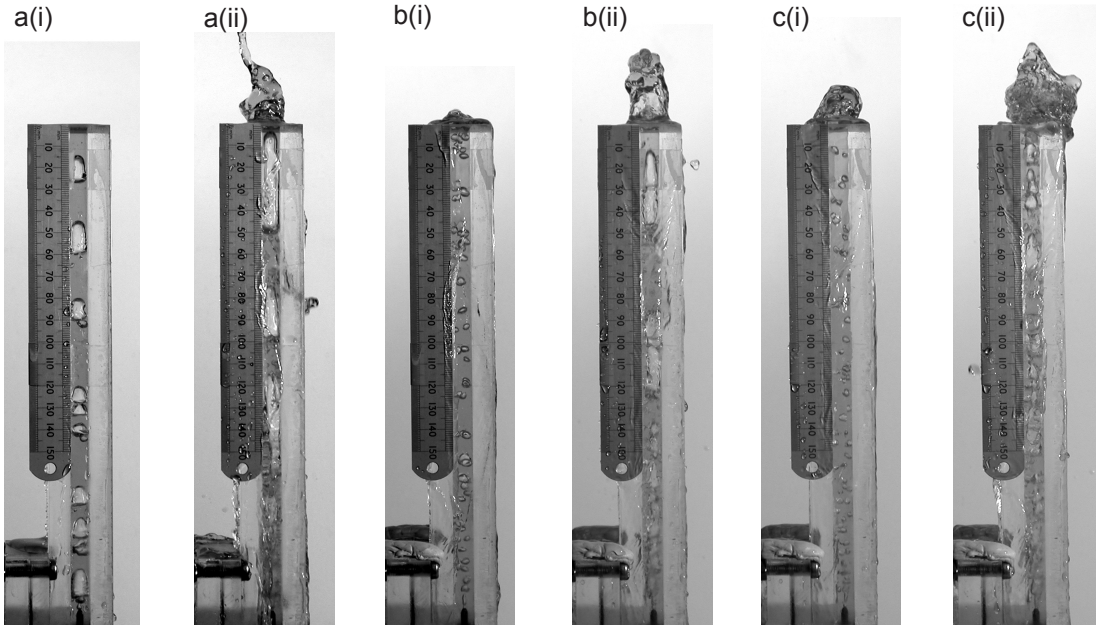

Figure 5, Woods et al., 2005

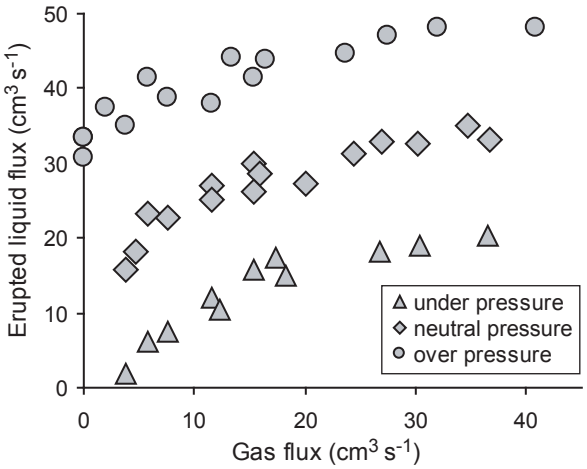

Figure 6, Woods et al., 2005

a(i)

a(ii)

b(i)

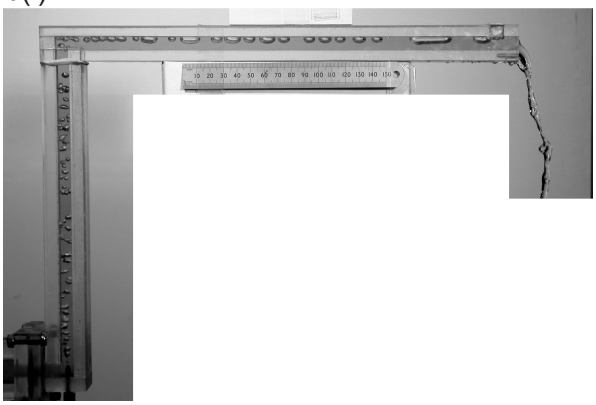

b(ii)

Figure 7, Woods et al., 2005

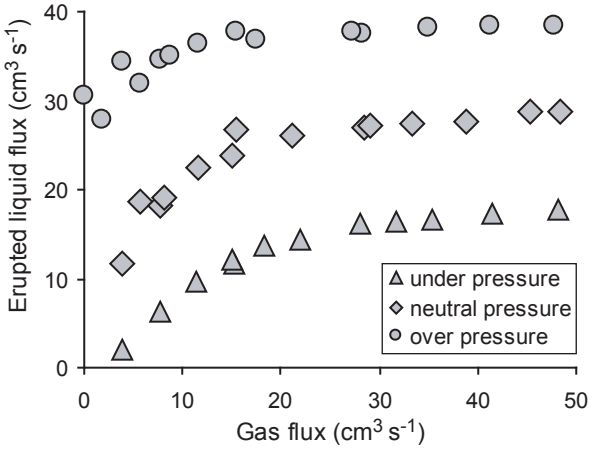

Figure 8, Woods et al., 2005

a

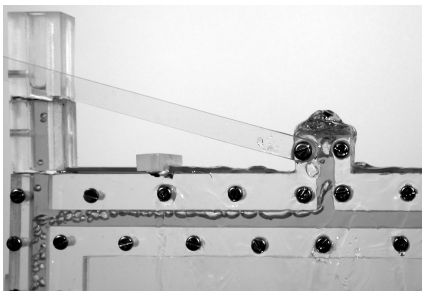

b

c

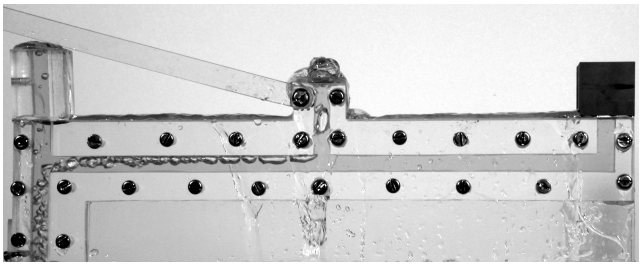

d

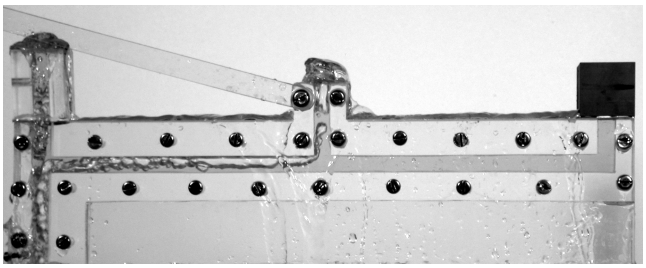

e

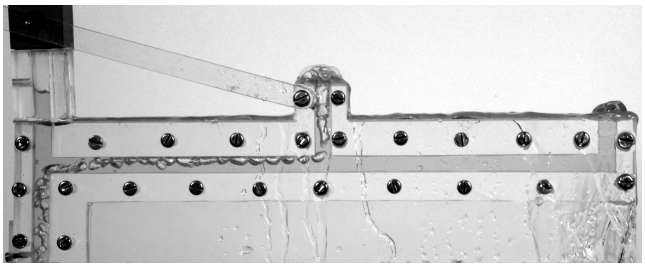

Figure 9, Woods et al., 2005

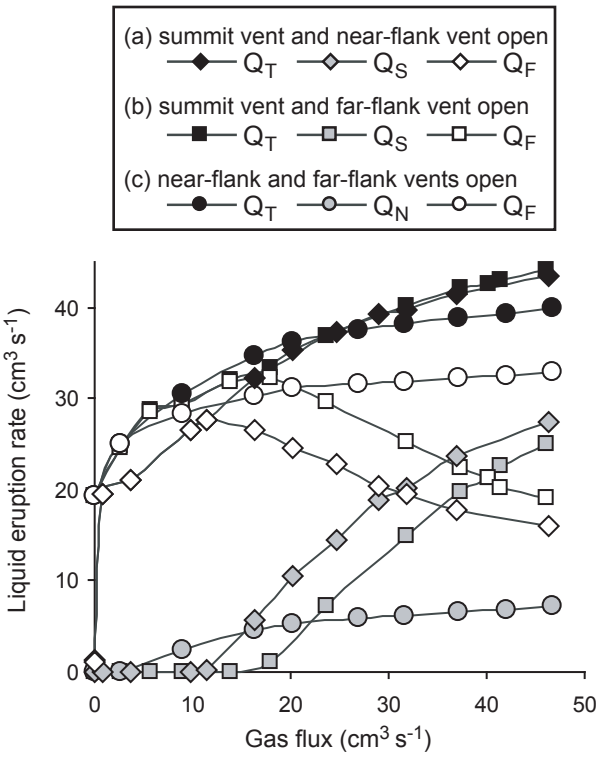

Figure 10, Woods et al., 2005

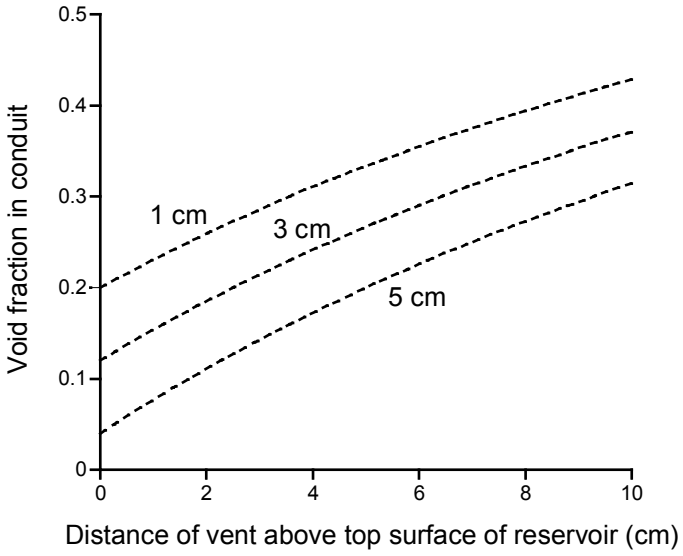

Figure 11, Woods et al., 2005

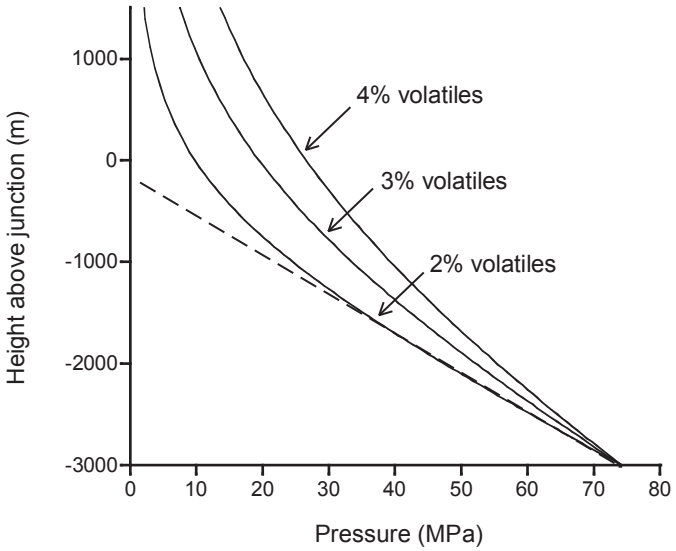

Figure 12, Woods et al., 2005

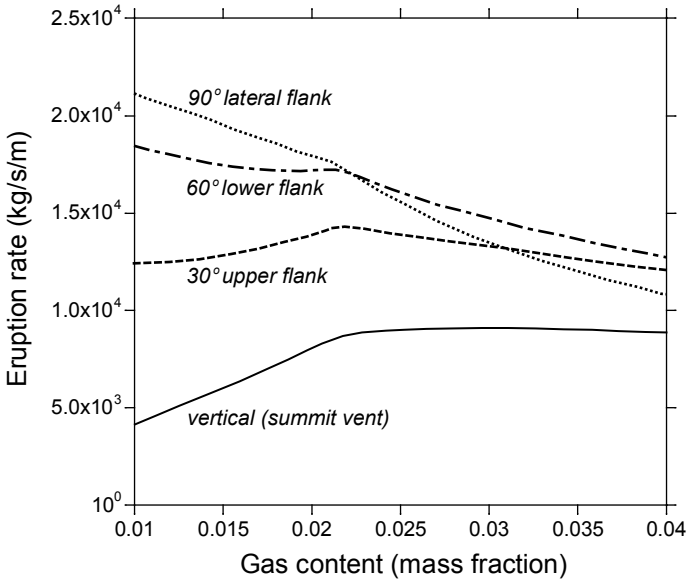

Figure 13, Woods et al., 2005